Published in final edited form as:
Biochem Pharmacol. 2012 June 15; 83(12): 1613–1622. doi:10.1016/j.bcp.2012.02.028.

GW583340 and GW2974, human EGFR and HER-2 inhibitors, reverse ABCG2- and ABCB1-mediated drug resistance

Kamlesh Sodani, **Amit K. Tiwari**, **Satyakam Singh**, **Atish Patel**, **Zhi-Jie Xiao**, **Jun-Jiang Chen**, **Yue-Li Sun**, **Tanaji T. Talele**, and **Zhe-Sheng Chen***
Department of Pharmaceutical Sciences, College of Pharmacy and Allied Health Professions, St. John's University, Queens, NY 11439, USA

Abstract

The overexpression of ATP binding cassette (ABC) transporters often leads to the development of multidrug resistance (MDR) and results in a suboptimal response to chemotherapy. Previously, we reported that lapatinib (GW572016), a human epidermal growth factor receptor (EGFR) and HER-2 tyrosine kinase inhibitor (TKI), significantly reverses MDR in cancer cells by blocking the efflux function of ABC subfamily B member 1 (ABCB1)- and ABC subfamily G member 2 (ABCG2)-mediated MDR. In the present study, we conducted *in vitro* experiments to evaluate if GW583340 and GW2974, structural analogues of lapatinib, could reverse ABCB1-and ABCG2-mediated MDR. Our results showed that GW583340 and GW2974 significantly sensitized ABCB1 and ABCG2 overexpressing MDR cells to their anticancer substrates. GW583340 and GW2974 significantly increased the intracellular accumulation of [^{3}H]-paclitaxel in ABCB1 overexpressing cells and [^{3}H]-mitoxantrone in ABCG2 overexpressing cells respectively. In addition, GW583340 and GW2974 significantly inhibited ABCG2-mediated transport of methotrexate in ABCG2 overexpressing membrane vesicles. There was no significant change in the expression levels of ABCB1 and ABCG2 in the cell lines exposed to 5 μM of either GW583340 or GW2974 for 3 days. In addition, a docking model predicted the binding conformation of GW583340 and GW2974 to be within the transmembrane region of homology modeled human ABCB1 and ABCG2. We conclude that GW583340 and GW2974, at clinically achievable plasma concentrations, reverse ABCB1- and ABCG2-mediated MDR by blocking the drug efflux function of these transporters. These findings may be useful in developing combination therapy for cancer treatment with EGFR TKIs.

Keywords

GW583340; GW2974; ABCB1; ABCG2; multidrug resistance; tyrosine kinase inhibitor

1 Introduction

Cancer chemotherapy typically involves use of combinations of anticancer drugs from different classes and with different mechanisms of action. However, cancer cells can become resistant to chemotherapy via a phenomenon known as multidrug resistance (MDR).

*Requests for reprints: Zhe-Sheng Chen, Department of Pharmaceutical Sciences, St. John's University, Queens, New York, 11439. Chenz@stjohns.edu, Phone: 1-718-990-1432, Fax: 1-718-990-1877.

One of the major mechanisms that produce the MDR phenotype is overexpression of ATP binding cassette (ABC) transporters. ABC transporters are transmembrane proteins that extrude a wide range of structurally and mechanistically diverse anticancer drugs against a concentration gradient, thereby producing chemotherapy failure [1]. Currently, 49 human ABC transporters have been identified and classified into seven different subfamilies (A-G) based on sequence similarities [2]. ABC subfamily B member 1 (ABCB1/P-gp), ABC subfamily C member 1 (ABCC1/MRP1) and ABC subfamily G member 2 [ABCG2, also known as breast cancer resistance protein (BCRP), mitoxantrone (MX) resistance protein (MXR) or placenta specific ABC protein (ABCP)] are the prime contributors of MDR in cancer cells [3,4]. ABC transporters also play a protective role by extruding xenobiotics and toxicants from normal cells [3,4]. In addition, ABC transporters are involved in transporting biologically important substrates across the cellular membranes, including amino acids, cholesterol and its derivatives, sugars, vitamins, peptides, lipids, some important proteins, hydrophobic drugs and antibiotics [3,5,6].

ABCB1, a 170 kDa transmembrane protein, can transport a wide range of substrates including hydrophobic anticancer drugs such as anthracyclines, vinca alkaloids, taxanes and epipodophyllotoxins [1,3]. ABCC1, a 190 kDa transmembrane protein, produces resistance to anthracyclines, taxanes, epipodophyllotoxins, vinca alkaloids and camptothecins [7]. ABCG2 is a 72 kDa half transporter which transports important anticancer drugs such as MX, camptothecins, anthracyclines, methotrexate (MTX) and flavopiridol through functional homodimer or heterodimer [8,9].

The human epidermal growth factor receptor (EGFR) is a member of HER/ErbB family of tyrosine kinase receptor [10]. The EGFR family of receptors regulates differentiation and morphology of cells and plays a pivotal role in organ development and growth. However, overexpression, dysregulation or mutation of EGFR leads to unrestricted and uncontrolled tumor growth and progression through several pathways including Ras/mitogen-activated protein kinase (MAPK), phosphatidylinositol 3-kinase (PI3K) and protein kinase C signaling cascade [10,11]. Recently, a number of EGFR tyrosine kinase inhibitors (TKIs) have been approved by FDA as therapy for different tumors. They exert their activity by competing with ATP for binding at the catalytic domain of the respective intracellular tyrosine kinases of EGFR receptors, thus blocking the intracellular signal transduction involved in the cancer development [12]. It is conceivable that TKI activity might be affected by the ATPase activity of ABC transporters. Interestingly, *in vitro* studies revealed that canertinib (CI-1033), an EGFR TKI, inhibited ABCG2 function and enhanced cytotoxicity of topotecan and SN-38 in cancer cells [13]. Gefitinib, an EGFR TKI, was reported to inhibit ABCB1- and ABCG2-mediated efflux activity in MCF-7/Adr and K562/BCRP cell line, respectively and thus reverse MDR [14,15]. Previously, we reported that erlotinib and AG1478, both are EGFR TKIs, and nilotinib, a BCR-ABL TKI, can antagonize ABCB1 and ABCG2 function *in vitro* [16-18]. Interestingly, lapatinib (Tykerb®; GW572016), an orally active, small molecule 4-anilinoquinazoline TKI, significantly augments the cytotoxic action of ABCB1 and ABCG2 substrates by reversing ABCB1- and ABCG2-mediated MDR in both *in vitro* and *in vivo* [19]. Lapatinib inhibits dual EGFR and HER-2 [20] and is currently being used in treatment of patients with advanced or metastatic breast cancer [21].

The analogues of lapatinib, GW583340 and GW2974, are small molecule quinazoline derivatives. They also exhibit dual EGFR/ErbB2 kinase inhibitory activity [22,23]. GW583340 is under clinical development and information about its anticancer activity and clinical data have not been published. GW2974 has been reported to have chemopreventive and therapeutic activity in gallbladder carcinoma and breast cancer [23,24]. It was reported that GW2974 has cardiac cell protective activity [25]. GW2974, as an anticancer drug, is not progressed to clinical trials because of some pharmacokinetic issues [24]. Until now, the

interaction of GW583340 and GW2974 compounds with ABC transporters has not been reported. This is the first report investigating the modulation of MDR transporters ABCB1, ABCC1 and ABCG2 activity by GW588340 and GW2974 with conventional anticancer drugs.

2 Materials and Methods

2.1 Chemicals

[^{3}H]-MX (4 Ci/mmol), [^{3}H]-paclitaxel (23 Ci/mmol) and [^{3}H]-MTX (24 Ci/mmol) were purchased from Moravek Biochemicals, Inc (Brea, CA). Dulbecco's modified Eagle's medium (DMEM), fetal bovine serum (FBS), penicillin/streptomycin and trypsin 0.25% were purchased from Hyclone (Waltham, MA). The monoclonal antibodies BXP-21 (against ABCG2), sc-8432 (against actin) and the secondary horseradish peroxidase-labeled anti-mouse IgG were purchased from Santa Cruz Biotechnology, Inc. (Santa Cruz, CA). The monoclonal antibody C219 (against ABCB1) was purchased from Abcam (Cambridge, MA). Fumitremorgin C (FTC) was synthesized by Thomas McCloud, Developmental Therapeutics Program, and Natural Products Extraction Laboratory, NIH (Bethesda, MD) and was a gift from Dr. Susan Bates. ONO-1078 (specific ABCC1 inhibitor) was a gift from Dr. Shin-ichi Akiyama (Sakuragaoka, Japan) [26]. GW583340 was purchased from Tocris Bioscience (Ellisville, MO). GW2974, MX, doxorubicin (DOX), colchicine, paclitaxel, vincristine, cisplatin, verapamil, (3-(4,5-dimethylthiazol-yl)-2,5-diphenyltetrazolium bromide (MTT), dimethyl sulfoxide (DMSO) and other chemicals were obtained from Sigma Chemical Co. (St. Louis, MO).

2.2 Cell lines

The KB-C2 cell line overexpressing ABCB1, was established by a step-wise exposure of KB-3-1, a parental human epidermoid carcinoma cell line, to increasing concentration of colchicine upto 2 μg/mL [27]. HEK293/pcDNA3.1 (parental), ABCG2-482-R2, and ABCG2-482-T7 cell lines were established by selection with G418 after transfecting HEK293 cell line with either an empty pcDNA3.1 vector or pcDNA3.1 vector containing a full length ABCG2 with either Arg or Thr at position 482, respectively, and were cultured in medium with 2 mg/mL of G418 [28]. The lung cancer cell line NCI-H460 (parental) and ABCG2 overexpressing NCI-H460/MX20 cells were kindly provided by Drs. Susan Bates and Robert Robey (NCI, NIH, Bethesda), *ABCB1*-transfected HEK/ABCB1 and *ABCC1*-transfected HEK/ABCC1 cell lines were kindly provided by Dr. Suresh Ambudkar (NCI, NIH, Bethesda). All cells were grown as adherent monolayer in drug-free culture media for more than 2 weeks before assay. All cell lines were cultured at 37°C with 5% CO_2 and DMEM containing 10% FBS and 1% penicillin/streptomycin.

2.3 Cytotoxicity determination by MTT assay

We used a modified MTT colorimetric assay to detect the sensitivity of cells to anticancer drugs *in vitro* [29]. Briefly, cells were harvested and resuspended at a final concentration of 6×10^3 cells/well for KB-3-1, HEK293/pcDNA3.1, HEK/ABCB1, NCI-H460, NCI-H460/MX20 and HEK/ABCC1 cells, and 6×10^3 cells/well for KB-C2, ABCG2-482-R2, and ABCG2-482-T7. Cells were seeded evenly into (160 μl/well) 96-well plate. After seeding cells in 160 μl medium in a 96-well plate and incubating for 24 h at 37°C, 20 μl of various concentrations of the appropriate anticancer drug were added (20 μl of fixed concentration of the reversal compounds were added one hour prior to the anticancer drugs). Subsequently the cells with anticancer drugs in DMEM supplemented with 10% FBS were incubated at 37°C for 72 h. After 72 h, 20 μl MTT (4 mg/ml) was added to each well. The plates were incubated at 37°C for 4 h. After this, the MTT/medium was removed from each well without disturbing the cells, and 100 μl of DMSO was added to each well. Finally, the absorbance

was read at 570 nm by Opsys microplate reader (Dynex Technologies, Chantilly, VA). The degree of resistance was calculated by dividing the IC_{50} for the MDR cells with or without inhibitors by that of the parental cells without inhibitor. The potential reversal agents used in this study were GW583340 and GW2974 at 2.5 and 5 μM. Verapamil and FTC were used at nontoxic concentration of 5 μM as a positive control for ABCB1 and ABCG2 overexpressing cell lines, respectively.

2.4 Drug accumulation assay

2.4.1 [^{3}H]-MX accumulation assay—The parental HEK293/pcDNA3.1, ABCG2-482-R2, and ABCG2-482-T7 cells were seeded in two T75 flasks and incubated with DMEM supplemented with 10% FBS at 37°C. After the cells reached 80% confluence, the cells were trypsinized and two aliquots (12×10^6 cells) from each cell line were suspended in the medium, pre-incubated with or without GW583340 or GW2974 (5 μM) at 37°C for 1 h. Subsequently, cells were suspended in the medium containing 0.1 μM [^{3}H]-MX with or without the reversal compound at 37°C for 2 h. The cells were washed with PBS for three times. Finally, the cells were lysed by adding lysis buffer (pH 7.4, containing 1% Triton X-100 and 0.2% SDS) and transferred to scintillation vial. Each sample was placed in scintillation fluid and radioactivity was measured in a Packard TRI-CARB® 1900CA liquid scintillation analyzer from Packard Instrument Company, Inc (Downers Grove, IL).

2.4.2 [^{3}H]-paclitaxel accumulation assay—The accumulation of [^{3}H]-paclitaxel in KB-3-1 and KB-C2 cells was measured in the presence or absence of GW583340, GW2974 or verapamil at 5 μM. Confluent cells in 24-well plates were preincubated with or without the reversal compounds for 1 h at 37°C. To measure drug accumulation, cells were then incubated with 0.1 μM [^{3}H]-paclitaxel for 2 h in the presence or absence of the reversal compounds at 37°C. After washing three times with ice cold PBS, the cells were trypsinized and placed in lysis buffer (pH 7.4, containing 1% Triton X-100 and 0.2% SDS). Each sample was placed in a scintillation vial with 5 mL scintillation fluid and radioactivity was measured in a Packard TRI-CARB1 1900CA liquid scintillation analyzer from Packard Instrument Company, Inc (Downers Grove, IL).

2.5 Inside-out vesicle uptake assay

For the uptake assay, we used HEK293/pcDNA3.1 and ABCG2 overexpressing ABCG2-482-R2 cell membrane vesicles. The experiment was carried out using a rapid filtration method, as previously described [30] in a medium containing membrane vesicles (10 μg), 0.25 M sucrose, 10 mM Tris-HCl, pH 7.4, 10 mM $MgCl_2$, 4 mM AMP/ATP, 10 mM phosphocreatine, 100 μg/ml creatine phosphokinase, and radio labeled substrate ([^{3}H]-MTX) with unlabeled substrate, in a total volume of 50 μl. Reactions were carried out at 37 °C for 10 minutes and was stopped by adding 3 ml of an ice-cold stop solution (0.25 M sucrose, 100 mM NaCl, 10 mM Tris-HCl, pH 7.4). Samples were passed through 0.22 μM Dura pore membrane filters (Millipore, Bedford, MA) under vacuum. The filters were washed three times with 3 ml of ice-cold stop solution and dried at room temperature for 30 min. Radioactivity was measured by the use of a liquid scintillation counter. The rates of net ATP-dependent transport were determined by subtracting the values obtained in the presence of 4 mM AMP from those obtained in the presence of 4 mM ATP.

2.6 Preparation of total cell lysates

Total cell lysates were prepared by harvesting the cells and rinsing twice with PBS. Cell extracts were prepared by incubating cells for 30 min with lysis buffer (10 mM Tris HCl, pH 7.5, 1 mM EDTA, 0.1% SDS, 150 mM NaCl, 1% Triton X-100 and 0.01% leupeptin) followed by centrifugation at 12,000 × g at 4 °C for 15 min. The supernatant containing total

cell lysates was stored at -80 °C until the gel electrophoresis was run. Protein concentrations were determined by bicinchonic acid (BCA™) based protein assay (Thermo Scientific, Rockford, IL).

2.7 Western blot analysis

Equal amounts of total cell lysates (80 μg protein) were resolved by sodium dodecyl sulfate polyacrylamide gel electrophoresis (SDS-PAGE) and electrophoretically transferred onto polyvinylidene fluoride (PVDF) membranes. After incubation in a blocking solution in TBST buffer (10 mM Tris–HCl, pH 8.0, 150 mM NaCl, and 0.1% Tween 20) for 1 h at room temperature, the membranes were immunoblotted overnight with primary monoclonal antibodies against either actin at 1:200 dilution or ABCB1 or ABCG2 at 1:200 dilution at 4 °C, and were then further incubated for 3 h at room temperature with horseradish peroxide (HRP)-conjugated secondary antibody (1:1000 dilution). The protein–antibody complex was detected by enhanced chemiluminescence detection system (Amersham, NJ). The protein expression was quantified by Scion Image Software (Scion Co., MD).

2.8 Molecular modeling

2.8.1 Ligand structure preparation—The structure of GW583340, GW2974 and the reference ligand lapatinib were built using the fragment dictionary of Maestro v9.0 and energy minimized by Macromodel program v9.7 (Schrödinger, Inc., New York, NY, 2009) using the OPLSAA force field with the steepest descent followed by truncated Newton conjugate gradient protocol. The low-energy 3D structure of GW583340, GW2974 and lapatinib were generated with the following parameters present in LigPrep v2.3: different protonation states at physiological pH±2, and all possible tautomers and ring conformations. Ligand structure obtained from the LigPrep run were further used for generating 100 ligand conformations for each protonated structure using the default parameters of mixed torsional/ low-mode sampling function. The conformations were filtered to exclude redundant conformers with a maximum relative energy difference of 5 kcal/mol. The output conformational search (Csearch) file containing 100 unique conformers for each ligand were used as input for docking simulations into each binding site of human ABCB1 and ABCG2.

2.8.2 Protein structure preparation—The X-ray crystal structure of ABCB1 in apoprotein state (PDB ID: 3G5U) and in complex with inhibitors QZ59-*RRR* (PDB ID: 3G60), QZ59-*SSS* (PDB ID: 3G61) [31] and ATP bound (PDB ID: 1MV5) obtained from the RCSB Protein Data Bank were used to build the homology model of human ABCB1. The protocol for homology modeling is essentially the same as reported before [32]. Refined human ABCB1 homology model was further used to generate different receptor grids by selecting QZ59-*RRR* (site-1) and QZ59-*SSS* (site-2) bound ligands, all amino acid residues known to contribute to verapamil binding (site-3), two residues (Phe728 and Val982) known to be common to sites 1-3 (site-4) and ATP binding site. Homology model of ABCG2 based on the mouse apoprotein (PDB ID: 3G5U) [31]; as template was generated previously by Rosenberg and Bikadi [33,34]. The homology model of ABCG2 was refined then the grid was generated using Arg482 as a centroid to dock the ligands. The choice of Arg482 as a centroid was further supported by performing site map v2.3 (Schrödinger, LLC, New York, NY, 2009) calculations, which has identified highest scoring druggable site (data not shown) encompassing Arg482 residue.

2.8.3 Docking protocol—Conformational libraries of GW583340, GW2974 and the reference ligand lapatinib were docked at each of the generated grids (site-1 to site-4 and ATP binding site of ABCB1, Arg482 residue for ABCG2) using the “Extra Precision” (XP) mode of Glide program v5.0 (Schrödinger, Inc., New York, NY, 2009) with the default functions. The top scoring GW583340 and GW2974 conformation with ABCB1 and

ABCG2 was used for graphical analysis. All computations were carried out on a Dell Precision 470n dual processor with the Linux OS (Red Hat Enterprise WS 4.0).

2.9 Statistical analysis

Differences of the parameters between two groups were analyzed by two tailed Student's *t* test. $P < 0.05$ was considered as statistically significant.

3 Results

3.1 GW583340 and GW2974 significantly potentiate the antineoplastic substrates of ABCG2 and ABCB1 transporters, but not of ABCC1 transporter

GW583340 and GW2974 were found to be nontoxic (with IC_{50} values of more than 100 μM) in ABCB1- and ABCG2-overexpressing cell lines when analyzed using the MTT assay (data not shown). Consequently, reversal concentration of 2.5 and 5 μM, at which no cytotoxicity was detected, were chosen for conducting reversal experiments. It has been established that mutations at position 482 in ABCG2 can alter the substrate and antagonist specificity of ABCG2 [35]. Therefore, we used both wild-type (R482) and mutant (R482T) forms of ABCG2 in the present study. The effect of GW583340 and GW2974 (2.5 and 5 μM) on ABCG2-mediated MDR in wild-type (ABCG2-482-R2) and mutant (ABCG2-482-T7) cell lines in combination with MX or DOX was determined. GW583340 and GW2974 significantly decreased the IC_{50} values of MX in both ABCG2-482-R2 and ABCG2-482-T7 cell lines in a concentration dependent manner (Table 1). In addition, the reversal effect produced by GW583340 at 5 μM was comparable to the effect produced by 5 μM of lapatinib and 5 μM of FTC (Table 1). Similar concentration dependent decrease in IC_{50} values for DOX in ABCG2 overexpressing ABCG2-482-R2 and ABCG2-482-T7 cell lines was obtained, when GW583340 or GW2974 (2.5 and 5 μM) was combined with DOX (Table 1). However, no change in the IC_{50} of cisplatin, a nonsubstrate of ABCG2, was seen with or without the combination of GW583340 and GW2974 at 5 μM (Table 1). In addition, the reversal effect was also analyzed in parental NCI-H460 and drug selected ABCG2 overexpressing NCI-H460/MX20 cells and a similar, concentration dependant reversal effect with GW583340 and GW2974 was noticed in NCI-H460/MX20 cells (Table.1). However, there was no significant alteration in the IC_{50} values of MX, DOX and cisplatin in the presence or absence of GW583340 and GW2974 in the HEK293/pcDNA3.1 and NCI-H460 cells (Table 1). Subsequently, the cell survival assay was done to determine whether both GW583340 and GW2974 could reverse ABCB1-mediated MDR by potentiating the sensitivity to substrate anticancer agents. GW583340 and GW2974 significantly increased the sensitivity of ABCB1 overexpressing drug selected KB-C2 and transfected HEK/ABCB1 cells to colchicine, vincristine and paclitaxel in a concentration-dependent fashion (Table 2). Lapatinib (GW572016), another TKI previously characterized by our laboratory [19] was used as a positive control. However, neither GW583340 nor GW2974 significantly altered the IC_{50} value of the aforementioned anticancer drugs in the parental KB-3-1 and HEK293/pcDNA3.1 cells (Table 2). In addition, GW583340 and GW2974 did not alter the IC_{50} value of cisplatin in KB-3-1, KB-C2, HEK293/pcDNA3.1 and HEK/ABCB1 cell line at concentration of 5 μM (Table 2). Verapamil, an ABCB1 inhibitor, at 5 μM, significantly decreased the IC_{50} values of colchicine, vincristine and paclitaxel in ABCB1 overexpressing KB-C2 and HEK/ABCB1 cell lines (Table 2). These results suggest that GW583340 and GW2974 significantly reverse the MDR mediated by ABCB1 or ABCG2. However, GW583340 and GW 2974, at 5 μM, did not significantly affect the ABCC1-mediated drug resistance in HEK/ABCC1 cell line (Table 3).

3.2 Effect of GW583340 or GW2974 on the cellular accumulation of [^{3}H]-MX and [^{3}H]-paclitaxel in cells overexpressing ABCG2 and ABCB1 respectively

Our MTT data suggested that GW583340 and GW2974 (2.5 and 5 μM) reversed ABCB1- and ABCG2-mediated MDR. However, the mechanism of reversal has not been elucidated. Therefore we determined the effect of GW583340 and GW2974 on the accumulation of anticancer substrates of ABCB1 and ABCG2 in cells overexpressing ABCB1 and ABCG2. The intracellular accumulation of [^{3}H]-MX, a known substrate of ABCG2, was measured in cells overexpressing ABCG2 in the presence or absence of 5 μM of GW583340 or GW2974 (Fig. 2A). These results indicated that GW583340 and GW2974 significantly increased the intracellular level of [^{3}H]-MX in cells overexpressing ABCG2. In addition, these results were comparable with FTC (5 μM), a known inhibitor of ABCG2 (Fig. 2A). However, neither GW583340 nor GW2974 significantly altered the intracellular level of [^{3}H]-MX in parental HEK293/pcDNA3.1 cells (Fig. 2A).

The intracellular accumulation of [^{3}H]-paclitaxel, a known substrate of ABCB1, was determined in KB-3-1 and KB-C2 cells in the presence or absence of 5 μM GW583340 or GW2974. As shown in Fig. 2B, the intracellular accumulation of [^{3}H]-paclitaxel was significantly low in ABCB1 overexpressing KB-C2 cells compared to parental KB-3-1 cells. GW583340 and GW2974 at 5 μM significantly increased the intracellular level of [^{3}H]-paclitaxel in KB-C2 cells (Fig. 2B). The increase in the intracellular level of [^{3}H]-paclitaxel in KB-C2 cells with GW583340 was comparable to 5 μM of verapamil (Fig. 2B). However, the intracellular level of [^{3}H]-paclitaxel in KB-3-1 cells was not significantly altered by GW583340, GW2974 or verapamil (Fig. 2B). These data suggested that GW583340 and GW2974 may block the drug efflux function of both ABCB1 and ABCG2, thus increasing intracellular levels of [^{3}H]-paclitaxel and [^{3}H]-MX in cells overexpressing ABCB1 and ABCG2, respectively.

3.3 Effect of GW583340 or GW2974 on uptake of [^{3}H]-MTX

To further elucidate the mechanism of the inhibitory effect of GW583340 and GW2974 on the transport activity of ABCG2, we determined the effect of these reversal compounds on [^{3}H]-MTX uptake in membrane vesicles prepared from ABCG2-482-R2 cells overexpressing ABCG2. Previously, we reported that wild-type ABCG2-482-R, but not mutant ABCG2-482-T7 membrane vesicles could transport [^{3}H]-MTX [30]. Thus, we determined the effect of GW583340 and GW2974 on the rate of ATP-dependent uptake of [^{3}H]-MTX by ABCG2 in the membrane vesicles prepared from parental HEK293/pcDNA3.1 and transfected ABCG2-482-R2 cells overexpressing ABCG2 (Fig. 3). GW583340 and GW2974, at 5 μM, significantly inhibited uptake of the [^{3}H]-MTX. Furthermore, the inhibitory effect of GW583340 and GW2974 at 5 μM on [^{3}H]-MTX transport by ABCG2 membrane vesicles was comparable to that of the positive control, FTC at 5 μM. These results suggested that GW583340 and GW2974 could inhibit the transport function of ABCG2.

3.4 Effect of GW583340 or GW2974 on the expression level of ABCG2 and ABCB1

ABCB1- and ABCG2-mediated MDR can be reversed either by decreasing ABCB1 and ABCG2 protein expression or by inhibiting their transport activity. To explore the reversal mechanism of GW583340 and GW2974, we incubated KB-C2 and ABCG2-482-R2 cells with GW583340 or GW2974 at 5 μM for 36 and 72 h. The results obtained from the Western blot analysis (Fig. 4) indicated no significant change in the protein expression levels of ABCB1 in KB-C2 cells or ABCG2 in ABCG2-482-R2 cells in the presence of GW583340 or GW2974. These results do not support our hypothesis that GW583340 or GW2974 affect the expression level of ABCB1 and ABCG2.

3.5 Binding model of GW583340 and GW2974 to ABCB1 and ABCG2

To understand the binding mechanism of GW583340 and GW2974 to a homology model of human ABCB1 [32] at the molecular level, we performed glide docking using ABCB1-QZ59-*RRR* (site-1), ABCB1-QZ59-*SSS* (site-2), ABCB1-verapamil (site-3), site common to above three sites (site-4) [31] and ATP binding site. For ABCG2, we used an Arg482 centered grid for docking as this residue has been previously reported to play a critical role in ligand binding through mutational experiments [28,36-38]. The binding energy (kcal/mol) data for the docked poses of GW583340, GW2974 and lapatinib at site-1 [-11.73, -9.41 and -11.54]; site-2 [-8.49, -5.98 and -8.05], site-3 [-5.14, -7.01 and -6.99], site-4 [-9.03, -7.85 and -7.40] and ATP-site [-5.00, -2.09 and -4.55] clearly indicated a QZ59-*RRR* binding site in ABCB1 i.e., site-1 as the most favorable site; hence, the following section will discuss bound conformation of GW583340 and GW2974 at site-1. The docking model of GW583340, GW2974 and Lapatinib with ABCG2 exhibited binding energy (kcal/mol) of -7.36, -5.41 and -7.62, respectively.

3.5.1 Model for binding of GW583340 to ABCB1—The XP-Glide predicted binding mode of GW583340 is shown in Fig. 5A. The hydrophobic portion of the methylsulfonylethane substituent present on the thiazole ring interacts with hydrophobic residues Met69, Phe72, Phe336 and Phe978. The thiazole ring is stabilized through hydrophobic interaction with Ala729, Phe732, and Leu975. The quinazoline ring forms hydrophobic contacts with the side chains of Phe336, Phe728 and Val982. The N_1 atom of the quinazoline ring is located such that it may form hydrogen bond with the side chains of both Tyr307 (-N---HO-Tyr307, 2.1 Å) and Gln725 (-N---H_2NOC-Gln725, 2.7 Å), thus restricting the number of degrees of freedom of these two residues. The chlorophenyl ring forms hydrophobic contacts with the side chains of Phe978, Val982 and Ala985. The fluorophenyl ring is extensively stabilized by the side chains of Ile864, Ile868, Met949, and Val981. The ether oxygen atom between the chlorophenyl and the fluorophenyl rings is located such that it may enter into hydrogen bonding interaction with the side chain hydroxyl group of Tyr953 (-O---HO-Tyr953, 2.8 Å).

3.5.2 Model for binding of GW583340 to ABCG2—The XP-Glide predicted binding model of GW583340 is shown in Fig. 5B. The methylsulfonylethane substituent present on the thiazole nucleus is stabilized through hydrophobic interactions with the side chains of Phe489, Leu581, Trp627 and Val631. The protonated amino group connected to the 2-position of the thiazole ring is involved in electrostatic interactions with the imidazole rings of each of the His630 residues protruding from each monomer. Through site-directed mutagenesis studies, it has been reported that His630 from each monomer play a critical role in function of ABCG2 [37]. The sulfur atom of the thiazole ring may form electrostatic interaction with the side chain of another critical residue Asn629 (-S---H_2NOC-Asn629, 3.2 Å) implicated in ABCG2 function [39]. The quinazoline ring forms hydrophobic contacts with the side chains of Phe507 and Met515. The fluorophenyl ring is extensively stabilized by the side chains of Phe489, Ile573 and Pro574. The fluoro substituent is located such that it may enter into hydrogen bonding interaction with the side chain of Tyr464 (-F---HO-Tyr464, 3.0 Å).

3.5.3 Model for binding of GW2974 to ABCB1—The XP-Glide predicted conformation of GW2974 within the drug binding cavity (site-1) of ABCB1 is shown in Fig. 6A. The pyridopyrimidine ring and dimethylamino group are located within the hydrophobic pocket formed by the side chains of Phe336, Phe728 and Val982. The N_1-atom of the pyrimidine ring may form a hydrogen bond with the side chains of both Tyr307 and Gln725 (-N---HO-Tyr307, 2.1 Å) and Gln725 (-N---H_2NOC-Gln725, 2.3 Å), which may lead to conformational restrictions of these two residues. The indazole ring is stabilized through

hydrophobic interaction with the side chains of Phe336, Leu975 and Val982. In addition, the phenyl portion of the indazole ring, being electron deficient, due the presence of two nitrogens, establishes a face to face arene-arene interaction with the side chain of Phe732. Moreover, the benzyl substituent at the N_1-position of the indazole ring is extensively stabilized through hydrophobic interactions with the side chains of Met69, Phe72, Phe336, Phe957 and Phe978.

3.5.4 Model for binding of GW2974 to ABCG2—The XP-Glide predicted conformation of GW2974 within the drug binding cavity of ABCG2 is shown in Fig. 6B. The dimethylamino group attached to the pyridopyrimidine ring is located within the hydrophobic pocket formed by the side chains of Ala580, Leu581 and Trp627. The pyridopyrimidine ring of GW2974 formed hydrophobic contacts with the side chains of Phe507, His630 and Leu633. The pyridine ring nitrogen atom may contribute towards electrostatic interaction through the side chain of Asn629 (-N---H_2N-Asn629, 3.7 Å). The -NH linker present between the pyridopyrimidine ring and the indazole ring may form electrostatic interaction with the nitrogen atom of the imidazole ring of His630 (-NH---N-His630, 3.5 Å). The indazole ring is stabilized through hydrophobic interaction with the side chains of Phe511 and His630. The benzyl substituent at the N_1-position of the indazole ring is stabilized through hydrophobic interactions with the side chains of Tyr464, Phe489, Ile573 and Pro574.

4 Discussion

GW583340 and GW2974 are quinazoline-derived compounds currently under clinical development. They bind to the ATP-binding site on tyrosine kinase domain of the EGFR and HER-2 and block the auto-phosphorylation of EGFR and HER-2 [22,23,40,41]. Previously, other quinazoline compounds, such as CI1033 and gefitinib, were shown to be substrates as well as inhibitors of ABCG2[13,42]. Recently, our group reported similar findings with other TKIs from the same class such as erlotinib, AG1478 and lapatinib (GW572016). These TKIs reverse ABCG2- and ABCB1-mediated MDR through inhibition of their efflux activity [16,17,19]. The interaction between ABC transporters and TKIs seems to be a class effect. *In vivo* studies from our group showed that lapatinib also augmented the anticancer activity of paclitaxel in ABCB1 overexpressing nude mouse xenograft model [19]. Furthermore, clinical data suggests that lapatinib interacts with ABC transporters [43]. In addition, lapatinib also has clinical benefit in patients with brain-metastasized breast cancer by increasing drug penetration across the blood brain barrier, presumably via inhibition of ABCB1 [43].

Our results showed for the first time that GW583340 and GW2974 significantly reverse ABCB1- and ABCG2-mediated MDR in a concentration-dependent fashion. GW583340 and GW2974 sensitized ABCB1 and ABCG2 overexpressing cells to their respective substrate anticancer drugs. Cytotoxicity data was also supported by accumulation studies, where both GW583340 and GW2974 significantly enhanced intracellular accumulation of [^{3}H]-MX in ABCG2 overexpressing cells and [^{3}H]-paclitaxel accumulation in ABCB1 overexpressing cells. GW583340 and GW2974 also inhibited transport of MTX in the ABCG2 membrane vesicle transport study. Overall, these results suggest that GW583340 and GW2974 interact with ABCG2 and inhibit ABCG2 activity. The incubation of ABCB1 and ABCG2 overexpressing cells with GW583340 or GW2974 did not alter the expression level of both ABCB1 and ABCG2, suggesting that the reversal effect of GW583340 and GW2974 result from the inhibition of the efflux function of ABCB1 and ABCG2.

Studies have shown that mutation at position 482 in ABCG2 (wild-type Arg^{482} to Gly ^{482} or Thr ^{482}) produce significant differences in the effectiveness of ABCG2 inhibitors as well as

the ability of ABCG2 to transport its substrate anticancer drugs [28,35]. Robey et al. have shown that these mutant cell lines have different transport efficacy, e.g., novobiocin blocks wild-type ABCG2 but is ineffective against mutants, while FTC can inhibit both wild-type as well as mutant ABCG2 [28]. Our results showed that GW583340 and GW2974 can inhibit the activity of both wild-type (R482) and mutant variant (R482T) of ABCG2. Several preclinical and clinical trials are exploring combination of EGFR TKIs with other anticancer drugs to improve chemotherapeutic outcome. EGFR TKIs may affect the pharmacokinetics of anticancer drugs, which may result in either increased response or increased adverse effects, especially in tissues where the concentration and distribution of anticancer drugs might be altered because of overexpression of ABCB1 and/or ABCG2. Therefore, interaction of these TKIs with ABCB1 and ABCG2 transporters should also be investigated. The peak plasma levels of lapatinib in humans are ≈ 3 μM and its half-life is ~ 17 h, with steady-state concentrations being achieved after six to seven days of once-daily dosing [44,45]. The lapatinib analogues used in our experiments may have reach similar plasma levels after therapeutic treatment. Thus, the concentration used in our *in vitro* experiment should be clinically achievable to sensitize refractory or resistant MDR cells through the inhibition of major MDR transporters such as ABCB1 and ABCG2.

To identify the binding interactions of GW583340 and GW2974 with ABCB1 and ABCG2 transporters, we performed molecular docking studies at various known sites of human ABCB1 and highest scored druggable site of ABCG2. The inhibition of ABCB1 and ABCG2 by the TKIs is considered to be a class effect that can be rationalized based on two criteria: a) in general, TKIs are hydrophobic (calculated logP value ranges from 3 to 6) and the drug binding site of ABCB1 and ABCG2 [46] is highly hydrophobic, and b) both ATP binding sites of EGFR TKs and transmembrane domains of human ABCB1 and ABCG2 are hydrophobic in nature. Moreover, the most potent compounds (GW583340 and lapatinib) appear to exhibit all of the pharmacophoric features such as hydrophobic groups and/or aromatic ring centers, hydrogen bond acceptors and positively charged ionizable group (secondary amine) that have been described as critical for ABCB1 and ABCG2 inhibition [47]. Ligand-based studies suggest the existence of an underlying correlation between ABCB1 inhibitory activity and lipophilicity of the compounds [48-50]. In this manner, GW583340 and lapatinib both showed QikProp derived ClogP value of 6.0 and 6.2, respectively, whereas the ClogP value for relatively less potent GW2974 was found to be 5.2. The greater ABCB1 and ABCG2 inhibitory activity of hydrophobic compounds may also be explained based on their ability to distribute within biomembrane from which ABCB1 and ABCG2 extracts these compounds. The lower efficacy of GW2974 may also be explained based on the lack of positively charged ionizable amine function in its structure. Recent site-directed mutagenesis study suggested that the mutation of two glutamine residues in the entry path of the ABCB1 transporter to positively charged arginine residue affected the inhibitory activity of positively charged group of propafenone analog through repulsion of positive-positive charge [51]. The binding energy scores expressed in kcal/mol for GW583340 and lapatinib against human ABCB1 [32] and ABCG2 [33,34] were found to be (-11.73 and -11.54) and (-7.36 and -7.62), respectively. Relatively lower binding energy score was noticed for GW2974 against ABCB1 (-9.41) and ABCG2 (-5.41), thus strengthening the applicability of human ABCB1 and ABCG2 homology models. GW2974, based on its reversal effect, is a rather weak inhibitor of ABCB1 and ABCG2, which could partially explain its poor binding energy score. Though docking is a useful tool in understanding ligand-protein interactions, the present study involves ABCB1 and ABCG2 which are particularly challenging since ABCB1 possesses a large drug binding cavity and ABCG2 may be active only in dimer or oligomer form. Currently, no high resolution crystal structures of human ABCB1 and ABCG2 are available and this prompted us to rely on homology models of human ABCB1 and ABCG2. Hence, the docking results should be interpreted with caution. Nevertheless, in the absence of co-crystal complexes of

GW583340- and GW2974-ABCB1 and -ABCG2, GW583340 and GW2974 docking model will form the basis for future optimization of 4-aminoquinazoline derivatives as inhibitors of ABCB1 and ABCG2.

In conclusion, this study is the first to report that both GW583340 and GW2974 reverse ABCB1- and ABCG2-mediated MDR by blocking their efflux function. These results suggest that GW583340 and GW2974 have the potential to be used in combination with conventional ABCB1 and ABCG2 substrate anticancer drugs to augment the response to chemotherapy.

Acknowledgments

We are thankful to Dr. Michael M. Gottesman (NCI, NIH, Bethesda, USA) for KB-3-1 cells, Shin-ichi Akiyama (Kagoshima University, Japan) for KB-C2 cell line and ONO-1078, Susan E. Bates and Robert W. Robey (NIH,USA) for FTC and *ABCG2*-transfected cell lines, ABCG2 drug selected NCI-H460/MX20, Dr. Suresh V. Ambudkar for *ABCB1*-transfected HEK/ABCB1 and *ABCC1*-transfected HEK/ABCC1 cell lines and for his critical comments in manuscript preparation. We thank Dr. Mark F. Rosenberg and Dr. Zsolt Bikadi (Manchester Interdisciplinary Biocentre, 131 Princess Street, University of Manchester, Manchester, M1 7DN, UK) for providing coordinates of ABCG2 homology model. We are thankful to Dr. Charles R. Ashby Jr. (St. John's University) for the critical review of the manuscript.

Grant Support: This work was supported by funds from NIH (No. 1R15CA143701) and St. John's University Research Seed Grant (No. 579-1110-7002) to Z.S. Chen.

References

1. Gottesman MM, Fojo T, Bates SE. Multidrug resistance in cancer: role of ATP-dependent transporters. Nat Rev Cancer. 2002; 2:48–58. [PubMed: 11902585]
2. Vasiliou V, Vasiliou K, Nebert DW. Human ATP-binding cassette (ABC) transporter family. Hum Genomics. 2009; 3:281–90. [PubMed: 19403462]
3. Dean M, Annilo T. Evolution of the ATP-binding cassette (ABC) transporter superfamily in vertebrates. Annu Rev Genomics Hum Genet. 2005; 6:123–42. [PubMed: 16124856]
4. Dean M, Rzhetsky A, Allikmets R. The human ATP-binding cassette (ABC) transporter superfamily. Genome Res. 2001; 11:1156–66. [PubMed: 11435397]
5. Gottesman MM, Ambudkar SV. Overview: ABC transporters and human disease. J Bioenerg Biomembr. 2001; 33:453–8. [PubMed: 11804186]
6. Goldstein LJ, Gottesman MM, Pastan I. Expression of the MDR1 gene in human cancers. Cancer Treat Res. 1991; 57:101–19. [PubMed: 1686712]
7. Kruh GD, Belinsky MG. The MRP family of drug efflux pumps. Oncogene. 2003; 22:7537–52. [PubMed: 14576857]
8. Doyle LA, Ross DD. Multidrug resistance mediated by the breast cancer resistance protein BCRP (ABCG2). Oncogene. 2003; 22:7340–58. [PubMed: 14576842]
9. Krishnamurthy P, Schuetz JD. Role of ABCG2/BCRP in biology and medicine. Annu Rev Pharmacol Toxicol. 2006; 46:381–410. [PubMed: 16402910]
10. Flynn JF, Wong C, Wu JM. Anti-EGFR Therapy: Mechanism and Advances in Clinical Efficacy in Breast Cancer. J Oncol. 2009; 2009:526963. [PubMed: 19390622]
11. Normanno N, De LA, Bianco C, Strizzi L, Mancino M, Maiello MR, Carotenuto A, De FG, Caponigro F, Salomon DS. Epidermal growth factor receptor (EGFR) signaling in cancer. Gene. 2006; 366:2–16. [PubMed: 16377102]
12. Lackey KE. Lessons from the drug discovery of lapatinib, a dual ErbB1/2 tyrosine kinase inhibitor. Curr Top Med Chem. 2006; 6:435–60. [PubMed: 16719802]
13. Erlichman C, Boerner SA, Hallgren CG, Spieker R, Wang XY, James CD, Scheffer GL, Maliepaard M, Ross DD, Bible KC, Kaufmann SH. The HER tyrosine kinase inhibitor CI1033 enhances cytotoxicity of 7-ethyl-10-hydroxycamptothecin and topotecan by inhibiting breast cancer resistance protein-mediated drug efflux. Cancer Res. 2001; 61:739–48. [PubMed: 11212277]

14. Kitazaki T, Oka M, Nakamura Y, Tsurutani J, Doi S, Yasunaga M, Takemura M, Yabuuchi H, Soda H, Kohno S. Gefitinib an EGFR tyrosine kinase inhibitor, directly inhibits the function of P-glycoprotein in multidrug resistant cancer cells. Lung Cancer. 2005; 49:337–43. [PubMed: 15955594]
15. Yanase K, Tsukahara S, Asada S, Ishikawa E, Imai Y, Sugimoto Y. Gefitinib reverses breast cancer resistance protein-mediated drug resistance. Mol Cancer Ther. 2004; 3:1119–25. [PubMed: 15367706]
16. Shi Z, Peng XX, Kim IW, Shukla S, Si QS, Robey RW, Bates SE, Shen T, Ashby CR Jr, Fu LW, Ambudkar SV, Chen ZS. Erlotinib (Tarceva, OSI-774) antagonizes ATP-binding cassette subfamily B member 1 and ATP-binding cassette subfamily G member 2-mediated drug resistance. Cancer Res. 2007; 67:11012–20. [PubMed: 18006847]
17. Shi Z, Tiwari AK, Shukla S, Robey RW, Kim IW, Parmar S, Bates SE, Si QS, Goldblatt CS, Abraham I, Fu LW, Ambudkar SV, Chen ZS. Inhibiting the function of ABCB1 and ABCG2 by the EGFR tyrosine kinase inhibitor AG1478. Biochem Pharmacol. 2009; 77:781–93. [PubMed: 19059384]
18. Tiwari AK, Sodani K, Wang SR, Kuang YH, Ashby CR Jr, Chen X, Chen ZS. Nilotinib (AMN107, Tasigna) reverses multidrug resistance by inhibiting the activity of the ABCB1/Pgp and ABCG2/BCRP/MXR transporters. Biochem Pharmacol. 2009; 78:153–61. [PubMed: 19427995]
19. Dai CL, Tiwari AK, Wu CP, Su XD, Wang SR, Liu DG, Ashby CR Jr, Huang Y, Robey RW, Liang YJ, Chen LM, Shi CJ, Ambudkar SV, Chen ZS, Fu LW. Lapatinib (Tykerb, GW572016) reverses multidrug resistance in cancer cells by inhibiting the activity of ATP-binding cassette subfamily B member 1 and G member 2. Cancer Res. 2008; 68:7905–14. [PubMed: 18829547]
20. Johnston SR, Leary A. Lapatinib: a novel EGFR/HER2 tyrosine kinase inhibitor for cancer. Drugs Today (Barc). 2006; 42:441–53. [PubMed: 16894399]
21. Schwartzberg LS, Franco SX, Florance A, O'Rourke L, Maltzman J, Johnston S. Lapatinib plus letrozole as first-line therapy for HER-2+ hormone receptor-positive metastatic breast cancer. Oncologist. 2010; 15:122–9. [PubMed: 20156908]
22. Aird KM, Ding X, Baras A, Wei J, Morse MA, Clay T, Lyerly HK, Devi GR. Trastuzumab signaling in ErbB2-overexpressing inflammatory breast cancer correlates with X-linked inhibitor of apoptosis protein expression. Mol Cancer Ther. 2008; 7:38–47. [PubMed: 18202008]
23. Kiguchi K, Ruffino L, Kawamoto T, Ajiki T, Digiovanni J. Chemopreventive and therapeutic efficacy of orally active tyrosine kinase inhibitors in a transgenic mouse model of gallbladder carcinoma. Clin Cancer Res. 2005; 11:5572–80. [PubMed: 16061875]
24. Witters LM, Witkoski A, Planas-Silva MD, Berger M, Viallet J, Lipton A. Synergistic inhibition of breast cancer cell lines with a dual inhibitor of EGFR-HER-2/neu and a Bcl-2 inhibitor. Oncol Rep. 2007; 17:465–9. [PubMed: 17203189]
25. Spector NL, Yarden Y, Smith B, Lyass L, Trusk P, Pry K, Hill JE, Xia W, Seger R, Bacus SS. Activation of AMP-activated protein kinase by human EGF receptor 2/EGF receptor tyrosine kinase inhibitor protects cardiac cells. Proc Natl Acad Sci U S A. 2007; 104:10607–12. [PubMed: 17556544]
26. Nagayama S, Chen ZS, Kitazono M, Takebayashi Y, Niwa K, Yamada K, Tani A, Haraguchi M, Sumizawa T, Furukawa T, Aikou T, Akiyama S. Increased sensitivity to vincristine of MDR cells by the leukotriene D4 receptor antagonist, ONO-1078. Cancer Lett. 1998; 130:175–82. [PubMed: 9751271]
27. Akiyama S, Fojo A, Hanover JA, Pastan I, Gottesman MM. Isolation and genetic characterization of human KB cell lines resistant to multiple drugs. Somat Cell Mol Genet. 1985; 11:117–26. [PubMed: 3856953]
28. Robey RW, Honjo Y, Morisaki K, Nadjem TA, Runge S, Risbood M, Poruchynsky MS, Bates SE. Mutations at amino-acid 482 in the ABCG2 gene affect substrate and antagonist specificity. Br J Cancer. 2003; 89:1971–8. [PubMed: 14612912]
29. Carmichael J, DeGraff WG, Gazdar AF, Minna JD, Mitchell JB. Evaluation of a tetrazolium-based semiautomated colorimetric assay: assessment of chemosensitivity testing. Cancer Res. 1987; 47:936–42. [PubMed: 3802100]

30. Chen ZS, Robey RW, Belinsky MG, Shchaveleva I, Ren XQ, Sugimoto Y, Ross DD, Bates SE, Kruh GD. Transport of methotrexate, methotrexate polyglutamates, and 17beta-estradiol 17-(beta-D-glucuronide) by ABCG2: effects of acquired mutations at R482 on methotrexate transport. Cancer Res. 2003; 63:4048–54. [PubMed: 12874005]

31. Aller SG, Yu J, Ward A, Weng Y, Chittaboina S, Zhuo R, Harrell PM, Trinh YT, Zhang Q, Urbatsch IL, Chang G. Structure of P-glycoprotein reveals a molecular basis for poly-specific drug binding. Science. 2009; 323:1718–22. [PubMed: 19325113]

32. Shi Z, Tiwari AK, Shukla S, Robey RW, Singh S, Kim IW, Bates SE, Peng X, Abraham I, Ambudkar SV, Talele TT, Fu LW, Chen ZS. Sildenafil reverses ABCB1- and ABCG2-mediated chemotherapeutic drug resistance. Cancer Res. 2011; 71:3029–41. [PubMed: 21402712]

33. Rosenberg MF, Bikadi Z, Chan J, Liu X, Ni Z, Cai X, Ford RC, Mao Q. The human breast cancer resistance protein (BCRP/ABCG2) shows conformational changes with mitoxantrone. Structure. 2010; 18:482–93. [PubMed: 20399185]

34. Hazai E, Bikadi Z. Homology modeling of breast cancer resistance protein (ABCG2). J Struct Biol. 2008; 162:63–74. [PubMed: 18249138]

35. Mao Q, Unadkat JD. Role of the breast cancer resistance protein (ABCG2) in drug transport. AAPS J. 2005; 7:E118–E133. [PubMed: 16146333]

36. Mitomo H, Kato R, Ito A, Kasamatsu S, Ikegami Y, Kii I, Kudo A, Kobatake E, Sumino Y, Ishikawa T. A functional study on polymorphism of the ATP-binding cassette transporter ABCG2: critical role of arginine-482 in methotrexate transport. Biochem J. 2003; 373:767–74. [PubMed: 12741957]

37. Miwa M, Tsukahara S, Ishikawa E, Asada S, Imai Y, Sugimoto Y. Single amino acid substitutions in the transmembrane domains of breast cancer resistance protein (BCRP) alter cross resistance patterns in transfectants. Int J Cancer. 2003; 107:757–63. [PubMed: 14566825]

38. Alqawi O, Bates S, Georges E. Arginine482 to threonine mutation in the breast cancer resistance protein ABCG2 inhibits rhodamine 123 transport while increasing binding. Biochem J. 2004; 382:711–6. [PubMed: 15139851]

39. Ni Z, Bikadi Z, Cai X, Rosenberg MF, Mao Q. Transmembrane helices 1 and 6 of the human breast cancer resistance protein (BCRP/ABCG2): identification of polar residues important for drug transport. Am J Physiol Cell Physiol. 2010; 299:C1100–C1109. [PubMed: 20739628]

40. Rusnak DW, Affleck K, Cockerill SG, Stubberfield C, Harris R, Page M, Smith KJ, Guntrip SB, Carter MC, Shaw RJ, Jowett A, Stables J, Topley P, Wood ER, Brignola PS, Kadwell SH, Reep BR, Mullin RJ, Alligood KJ, Keith BR, Crosby RM, Murray DM, Knight WB, Gilmer TM, Lackey K. The characterization of novel, dual ErbB-2/EGFR, tyrosine kinase inhibitors: potential therapy for cancer. Cancer Res. 2001; 61:7196–203. [PubMed: 11585755]

41. Cockerill S, Stubberfield C, Stables J, Carter M, Guntrip S, Smith K, McKeown S, Shaw R, Topley P, Thomsen L, Affleck K, Jowett A, Hayes D, Willson M, Woollard P, Spalding D. Indazolylamino quinazolines and pyridopyrimidines as inhibitors of the EGFr and C-erbB-2. Bioorg Med Chem Lett. 2001; 11:1401–5. [PubMed: 11378364]

42. Elkind NB, Szentpetery Z, Apati A, Ozvegy-Laczka C, Varady G, Ujhelly O, Szabo K, Homolya L, Varadi A, Buday L, Keri G, Nemet K, Sarkadi B. Multidrug transporter ABCG2 prevents tumor cell death induced by the epidermal growth factor receptor inhibitor Iressa (ZD1839, Gefitinib). Cancer Res. 2005; 65:1770–7. [PubMed: 15753373]

43. Midgley RS, Kerr DJ, Flaherty KT, Stevenson JP, Pratap SE, Koch KM, Smith DA, Versola M, Fleming RA, Ward C, O'Dwyer PJ, Middleton MR. A phase I and pharmacokinetic study of lapatinib in combination with infusional 5-fluorouracil, leucovorin and irinotecan. Ann Oncol. 2007; 18:2025–9. [PubMed: 17846021]

44. Burris HA III, Hurwitz HI, Dees EC, Dowlati A, Blackwell KL, O'Neil B, Marcom PK, Ellis MJ, Overmoyer B, Jones SF, Harris JL, Smith DA, Koch KM, Stead A, Mangum S, Spector NL. Phase I safety, pharmacokinetics, and clinical activity study of lapatinib (GW572016), a reversible dual inhibitor of epidermal growth factor receptor tyrosine kinases, in heavily pretreated patients with metastatic carcinomas. J Clin Oncol. 2005; 23:5305–13. [PubMed: 15955900]

45. Bence AK, Anderson EB, Halepota MA, Doukas MA, DeSimone PA, Davis GA, Smith DA, Koch KM, Stead AG, Mangum S, Bowen CJ, Spector NL, Hsieh S, Adams VR. Phase I pharmacokinetic

studies evaluating single and multiple doses of oral GW572016, a dual EGFR-ErbB2 inhibitor, in healthy subjects. Invest New Drugs. 2005; 23:39–49. [PubMed: 15528979]

46. Nicolle E, Boumendjel A, Macalou S, Genoux E, hmed-Belkacem A, Carrupt PA, Di PA. QSAR analysis and molecular modeling of ABCG2-specific inhibitors. Adv Drug Deliv Rev. 2009; 61:34–46. [PubMed: 19135106]
47. Ecker, GF.; Chiba, P. Transporters as Drug Carriers. WILEY-VCH; 2009.
48. Klopman G, Shi LM, Ramu A. Quantitative structure-activity relationship of multidrug resistance reversal agents. Mol Pharmacol. 1997; 52:323–34. [PubMed: 9271356]
49. Crivori P, Reinach B, Pezzetta D, Poggesi I. Computational models for identifying potential P-glycoprotein substrates and inhibitors. Mol Pharm. 2006; 3:33–44. [PubMed: 16686367]
50. Pajeva IK, Globisch C, Wiese M. Combined pharmacophore modeling, docking, and 3D QSAR studies of ABCB1 and ABCC1 transporter inhibitors. ChemMedChem. 2009; 4:1883–96. [PubMed: 19768722]
51. Parveen Z, Stockner T, Bentele C, Pferschy S, Kraupp M, Freissmuth M, Ecker GF, Chiba P. Molecular dissection of dual pseudosymmetric solute translocation pathways in human P-glycoprotein. Mol Pharmacol. 2011; 79:443–52. [PubMed: 21177413]

Abbreviations

MDR	multidrug resistance
ABC	ATP-binding cassette
ABCB1 (P-gp)	P-glycoprotein
ABCG2	also called BCRP (breast cancer resistance protein)/MXR (mitoxantrone resistance protein)
ABCC1 (MRP1)	multidrug resistance protein 1
EGFR	epidermal growth factor receptor
HER2	human epidermal growth factor receptor 2
TKI	tyrosine kinase inhibitor
PBS	phosphate-buffered saline
FTC	Fumitremorgin C

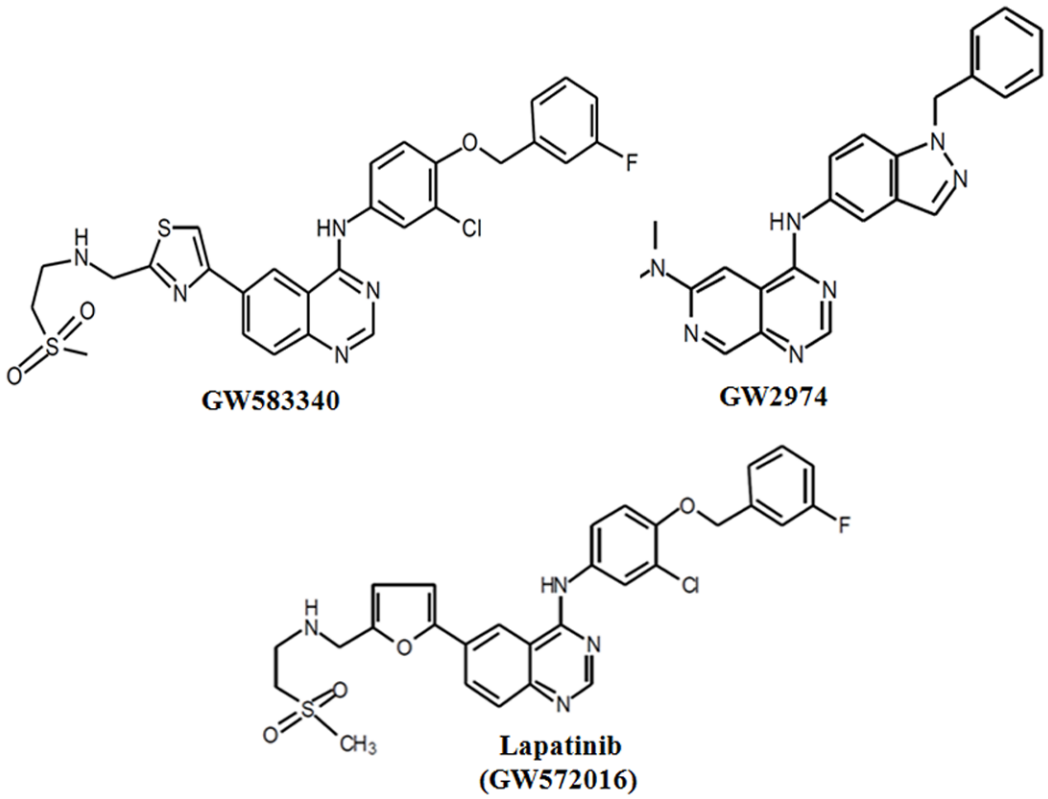

Fig. 1. Chemical structure of GW583340, GW2974 and lapatinib (GW572016)

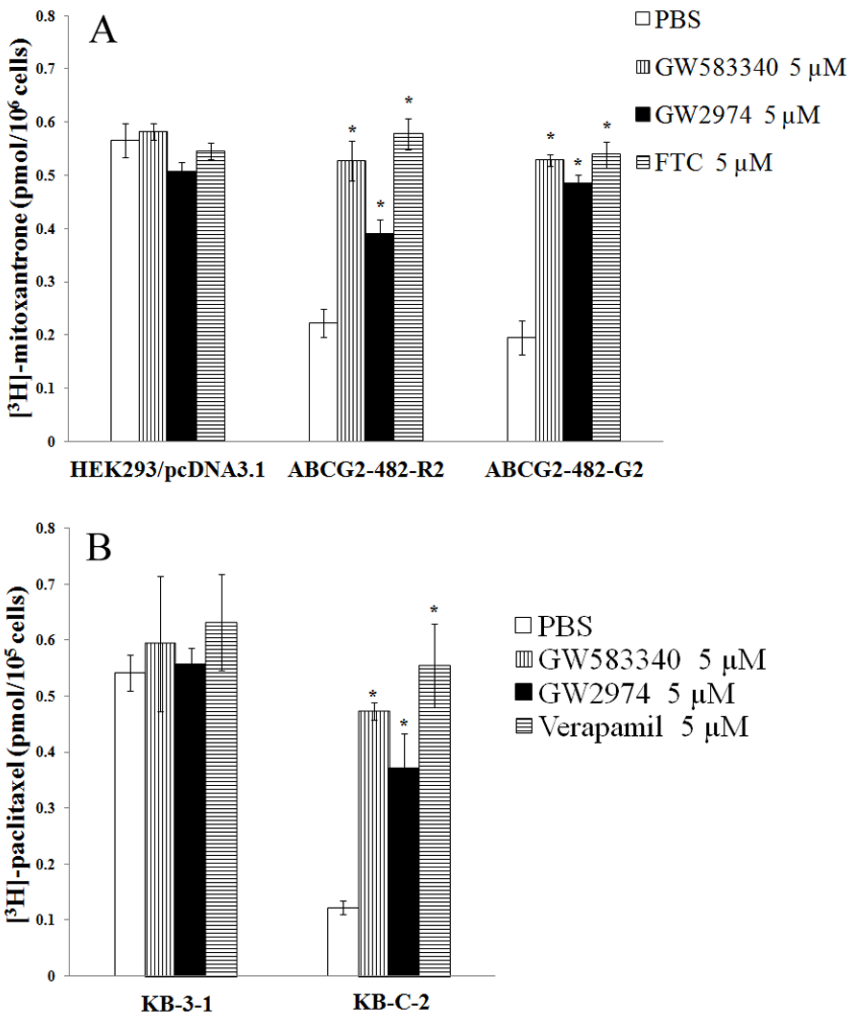

Fig. 2. Effect of GW583340 or GW2974 on the accumulation of [^{3}H]-MX and [^{3}H]-paclitaxel

The accumulation [^{3}H]-MX (A) in empty vector transfected HEK293/pcDNA3.1, *ABCG2* vector transfected wild-type ABCG2-482-R2, and mutant ABCG2-482-T7 or [^{3}H]-paclitaxel (B) in parental KB-3-1 and ABCB1 overexpressing KB-C2 cells was measured as described in Materials and Methods. Columns are the mean of triplicate determinations; bars, SD. *, $P < 0.05$ versus the control group. Experiments were done three independent times, and a representative experiment is shown.

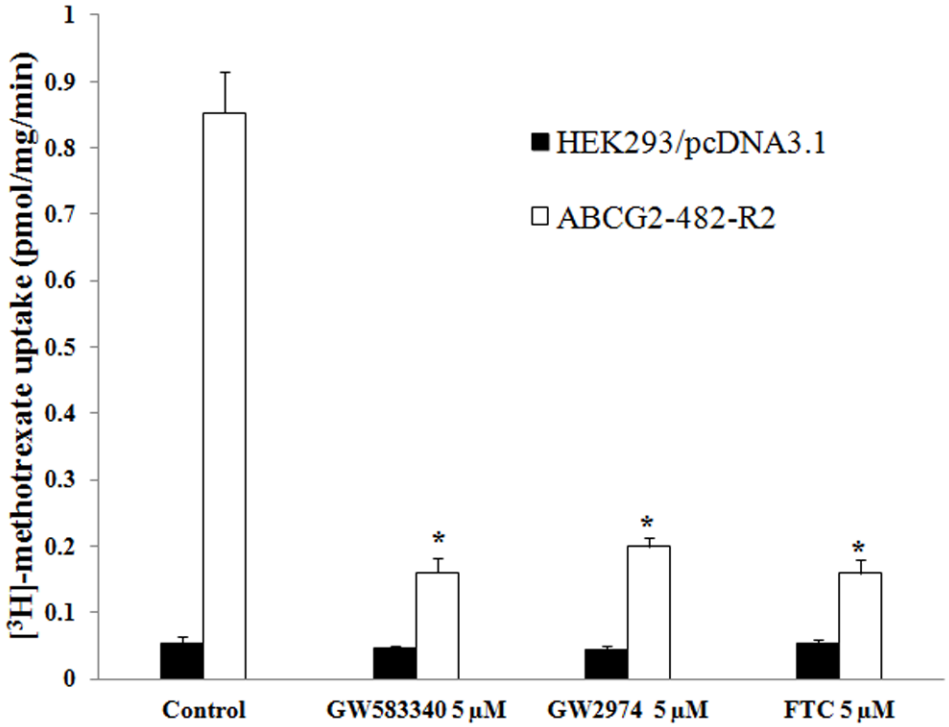

Fig. 3. Effect of GW583340 or GW2974 on the transport of [^{3}H]-MTX by ABCG2

The rates of the uptake [^{3}H]-MTX into membrane vesicles prepared from /pcDNA3.1 andABCG2-482-R2 cells were measured as described in Materials and Methods. Columns are the mean of triplicate determinations; bars, SD. *, $P < 0.01$, versus the control group. Experiments were done three independent times, and a representative experiment is shown.

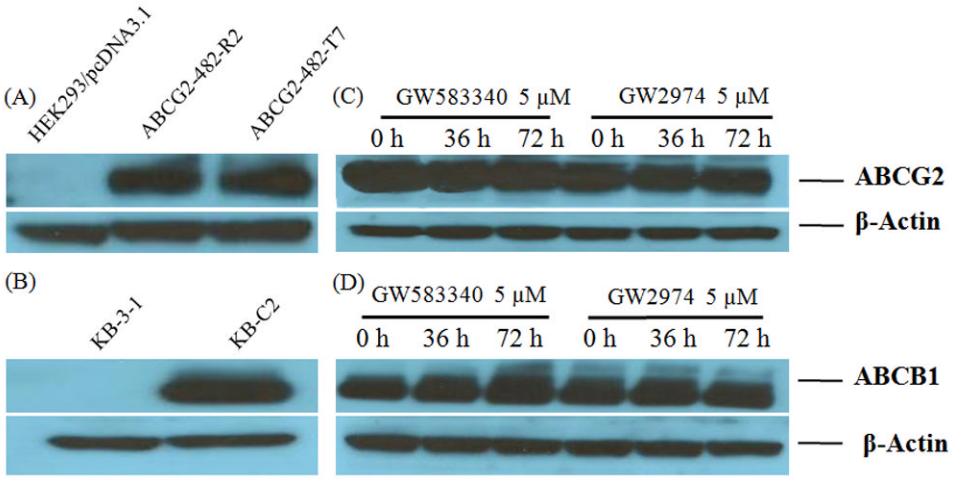

Fig. 4. Western blot analysis of ABCG2 and ABCB1, the effect of GW583340 or GW2974 on ABCG2 and ABCB1 expression

(A) Expression of ABCG2 in HEK293/pcDNA3.1, ABCG2-482-R2 and ABCG2-482-T7 cells. (B) Expression of ABCB1 in KB-3-1 and KB-C2 cells. (C) Effect of GW583340 and GW2974 at 5 μM on expression level of ABCG2 in ABCG2-482-R2 cells for 36 and 72 h. (D) Effect of GW583340 and GW2974 at 5 μM on the expression level of ABCB1 in KB-C2 cells for 36 h and 72 h.

Equal amounts of total cell lysate were used for each sample. Western blotting performed as described in Materials and Methods. Representative result is shown here and similar results were obtained in two other trials.

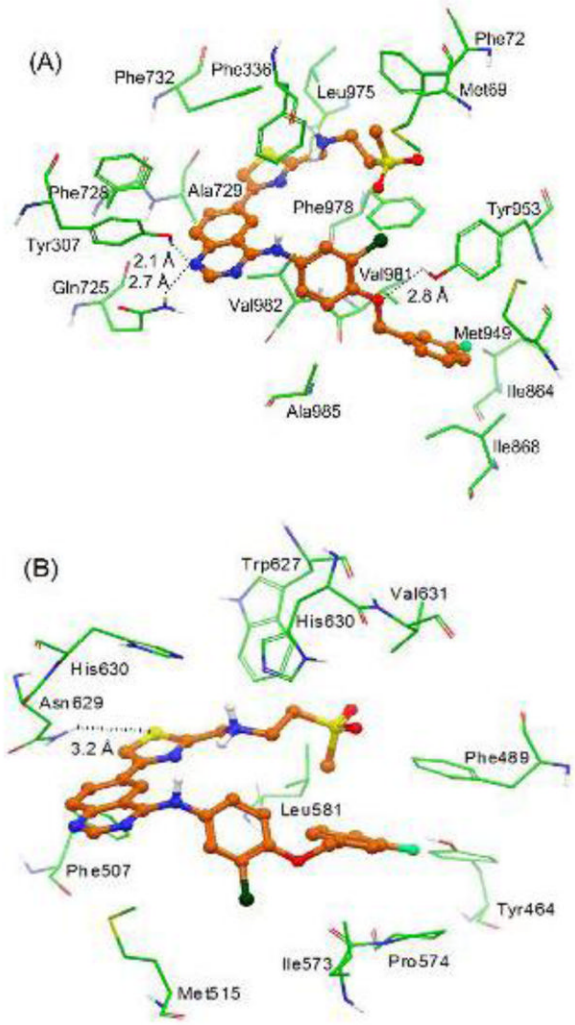

Fig. 5. XP-Glide predicted binding mode of GW583340 with homology modeled ABCB1 (panel A) and ABCG2 (panel B)

Important amino acids are depicted as sticks with the atoms colored as carbon – green, hydrogen – white, nitrogen – blue, oxygen – red, sulfur – yellow whereas the inhibitor is shown as ball and stick model with the same color scheme as above except carbon atoms are represented in orange, fluorine-light green and chlorine-dark green.

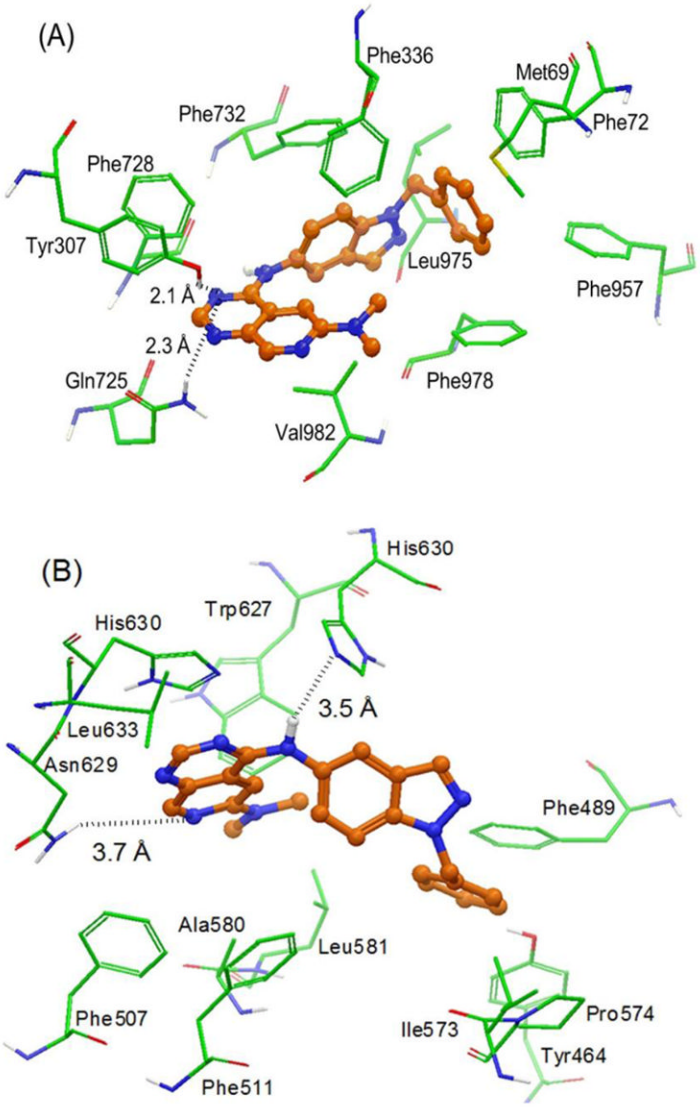

Fig. 6. XP-Glide predicted binding mode of GW2974 with homology modeled ABCB1 (panel A) and ABCG2 (panel B)

The color scheme is same as that of Fig. 5.

Table 1

GW583340 and GW2974 reverse the ABCG2-mediated drug resistance to mitoxantrone, doxorubicin and cisplatin.

Treatments	IC_{50} ± SD[a] (nM)					
	HEK 293/pcDNA3.1	(RF)[b]	ABCG2-482-R2	(RF)[b]	ABCG2-482-T7	(RF)[b]
Mitoxantrone (μM)	48.2 ± 5.9	1.0	651.8 ± 86.8	13.5	965.4 ± 135.7	20.0
+GW583340 - 2.5μM	47.6 ± 6.2	1.0	163.3 ± 23.7 *	3.4	218.2 ± 23.6 *	4.5
+GW583340 - 5μM	45.7 ± 4.9	0.9	74.8 ± 8.2 *	1.6	75.5 ± 8.9 *	1.6
+GW2974 - 2.5μM	46.8 ± 8.3	1.0	256.5 ± 26.4 *	5.3	345.4 ± 35.4 *	7.2
+GW2974 - 5μM	45.9 ± 4.7	0.9	122.3 ± 9.6 *	2.5	126.7 ± 16.4 *	2.6
+Lapatinib - 5μM	47.6 ± 9.6	1.0	72.1 ± 2.6 *	1.5	69.1 ± 7.9 *	1.4
+FTC - 5μM	41.2 ± 3.7	0.8	63.1 ± 3.5 *	1.3	58.4 ± 3.4 *	1.2
Doxorubicin (μM)	79.2 ± 3.2	1.0	578.3 ± 35.6	7.3	959.2 ± 159.6	12.1
+GW583340 - 2.5μM	76.5 ± 4.6	1.0	234.2 ± 19.8 *	2.9	183.2 ± 22.6 *	2.3
+GW583340 - 5μM	75.2 ± 13.5	0.9	167.2 ± 9.3 *	2.1	104.2 ± 8.1 *	1.3
+GW2974 - 2.5μM	82.1 ± 10.6	1.0	310.6 ± 48.6 *	3.9	241.4 ± 12.8 *	3.0
+GW2974 - 5μM	77.8 ± 6.8	1.0	201.8 ± 16.5 *	2.5	168.9 ± 6.4 *	2.1
+FTC - 5μM	75.6 ± 5.6	1.0	134.1 ± 8.4 *	1.7	95.7 ± 5.3 *	1.2
Cisplatin (μM)	1890.4 ± 126.8	1.0	1964.1 ± 163.4	1.0	1980.6 ± 146.3	1.0
+GW583340 - 5μM	1987.5 ± 156.8	1.1	1851.7 ± 182.6	1.0	2041.7 ± 124.6	1.1
+GW2974 - 5μM	1783.7 ± 108.9	0.9	1927.5 ± 196.7	1.0	1887.2 ± 157.6	1.0
+FTC - 5μM	1696.3 ± 148.8	0.9	2108.2 ± 216.8	1.1	1784.7 ± 196.3	0.9
	NCI-H460	(RF)[b]	NCI-H460/MX-20			(RF)[b]
Mitoxantrone	78.1 ± 8.2	1.0	17536.8 ± 3723.4			224.8
+GW583340 - 5μM	72.4 ± 14 .1	0.9	264.4 ± 21.2 *			3.4
+GW2974 - 5μM	68.7 ± 9.3	0.9	500.7 ± 68.8 *			6.4
+FTC - 5μM	71.5 ± 11.2	0.7	230.1 ± 19.9 *			3.0
Doxorubicin	95.2 ± 17.3	1.0	8674.8 ± 622.4			91.3

Treatments	IC_{50} ± SD[a] (nM)					
	HEK 293/pcDNA3.1	(RF)[b]	ABCG2-482-R2	(RF)[b]	ABCG2-482-T7	(RF)[b]
+GW583340 - 5μM	89.6 ± 13.5	0.9	296.5 ± 32.5 *			3.1
+GW2974 - 5μM	83.7 ± 6.2	0.9	646.6 ± 56.3 *			6.8
+FTC - 5μM	81.2 ± 8.5	0.9	241.2 ± 46.4 *			2.5
Cisplatin	980.5 ± 76.4	1.0	946.6 ± 64.8			1.0
+GW583340 - 5μM	955.3 ± 39.8	1.0	904.8 ± 120.4			0.9
+GW2974 - 5μM	854.7 ± 62.8	0.9	912.6 ± 73.7			0.9
+FTC - 5μM	838.1 ± 45.2	0.9	838.2 ± 91.3			0.9

[a] IC_{50} values are represented as mean ± SD of three independent experiments performed in triplicate.

[b] Values represent the resistance fold (RF) obtained by dividing IC_{50} value of antineoplastic drugs for HEK293/pcDNA3.1, ABCG2-482-R2 or ABCG2-482-T7 cells with or without reversal agent divided by the IC_{50} value of respective antineoplastic drug for HEK293/pcDNA3.1 cells without reversal agent. Resistance fold for NCI-H460 and NCI-H460/MX20 cells represented in the parenthesis was obtained in the similar fashion. Cell survival assay was determined by the MTT assay as described in Materials and Methods.
FTC was used as a positive control of ABCG2 inhibitor.

* $P < 0.05$ versus the control group.

Table 2

GW583340 and GW2974 reverse the ABCB1-mediated drug resistance to colchicine, paclitaxel, vincristine and cisplatin.

Treatments	IC_{50} ± SD[a] (nM)			
	HEK293/pcDNA3.1	(RF)[b]	HEK/ABCB1	(RF)[b]
Vincristine	13.9 ± 2.3	1.0	138.2 ± 8.8	9.9
+ GW583340 - 5 μM	11.2 ± 1.4	0.8	17.4 ± 4.6 *	1.3
+ GW2974 - 5 μM	10.4 ± 1.9	0.7	37.2 ± 3.8 *	2.7
+ Verapamil - 5 μM	9.8 ± 2.5	0.7	16.2 ± 3.5 *	1.2
Paclitaxel	26.4 ± 6.3	1.0	184.4 ± 23.2	7.0
+ GW583340 - 5 μM	23.2 ± 3.3	0.9	32.6 ± 5.2 *	1.2
+ GW2974 - 5 μM	22.8 ± 3.8	0.9	43.4 ± 6.4 *	1.6
+ Verapamil - 5 μM	23.1 ± 2.3	0.9	29.7 ± 4.3 *	1.1
Cisplatin	942.6 ± 63.9	1.0	987.3 ± 73.3	1.1
+ GW583340 - 5 μM	882.2 ± 47.4	0.9	839.19 ± 20.4	0.9
+ GW2974 - 5 μM	922.8 ± 23.9	1.0	884.0 ± 32.7	0.9
+ Verapamil - 5 μM	946.7 ± 42.8	1.0	923.7 ± 63.6	1.0
	KB-3-1	(RF)[b]	KB-C2	(RF)[b]
Colochicine	8.1 ± 2.6	1.0	3418.2 ± 342.1	422.0
+GW583340 - 2.5 μM	7.3 ± 1.5	0.9	694.5 ± 135.6 *	85.7
+GW583340 -5 μM	7.1 ± 0.6	0.9	194.8 ± 26.8 *	24.0
+GW2974 - 2.5 μM	7.2 ± 3.5	0.9	1647.2 ± 263.4*	203.0
+GW2974 - 5 μM	7.3 ± 1.9	0.9	894.2 ± 193.4 *	110.0
+Lapatinib - 5 μM	7.6 ± 2.5	0.9	184.3 ± 16.4 *	22.8
+Verapamil - 5 μM	6.3 ± 0.9	0.8	173.4 ± 18.9 *	21.4
Paclitaxel	8.4 ± 2.1	1.0	2559.1 ± 537.9	304.0
+GW583340 - 2.5 μM	7.6 ± 3.8	0.9	567.2 ± 168.7 *	67.5
+GW583340 - 5 μM	7.4 ± 0.9	0.9	276.2 ± 68.7 *	32.9
+GW2974 - 2.5 μM	7.9 ± 2.6	0.9	982.1 ± 267.9 *	117.0
+GW2974 - 5 μM	7.7 ± 1.1	0.9	498.2 ± 97.9 *	59.3
+Verapamil - 5 μM	7.6 ± 0.8	0.9	249.1 ± 19.8 *	29.7
Cisplatin	1807.1 ± 256.8	1.0	1866.7 ± 156.7	1.0
+GW583340 - 5 μM	1771.9 ± 98.6	1.0	1733.4 ± 216.2	1.0
+GW2974 - 5 μM	1813.6 ± 167.9	1.0	1896.6 ± 116.8	1.0
+Verapamil - 5 μM	1747.8 ± 158.1	1.0	1811.4 ± 216.3	1.0

[a] IC_{50} values are represented as mean ± SD of three independent experiments performed in triplicate.

[b] Values represent the resistance fold (RF) obtained by dividing IC_{50} value of antineoplastic drugs for KB-3-1 and KB-C2 cells with or without reversal agent divided by the IC_{50} value of respective antineoplastic drug for KB-3-1 cells without reversal agent. Resistance fold for HEK293/pcDNA3.1 and HEK/ABCB1 cells represented in the parenthesis was obtained in the similar fashion. Cell survival assay was determined by the MTT assay as described in Materials and Methods. Verapamil was used as a positive control of ABCB1 inhibitor.

[*] $P < 0.05$ versus the control group.

Table 3

GW583340 and GW2974 do not alter the ABCC1-mediated drug resistance to vincristine.

Treatments	IC_{50} ± SD[a] (nM)			
	HEK293/pcDNA3.1	(RF)[b]	HEK/MRP1	(RF)[b]
Vincristine	12.89 ± 2.83	1.0	89.08 ± 2.92	6.9
+ GW583340 - 5 μM	13.93 ± 3.74	1.1	83.24 ± 12.43	6.5
+ GW2974 - 5 μM	11.66 ± 4.82	0.9	78.40 ± 8.94	6.1
+ ONO-1078 10 μM	9.90 ± 1.03	0.8	19.63 ± 3.34*	1.5

[a] IC_{50} values are represented as mean ± SD of three independent experiments performed in triplicate.

[b] Values represent the resistance fold (RF) obtained by dividing IC_{50} value of antineoplastic drugs for HEK293/pcDNA3.1 and HEK/ABCC1 cells with or without reversal agent divided by the IC_{50} value of respective antineoplastic drug for HEK293/pcDNA3.1 cells without reversal agent. Cell survival assay was determined by the MTT assay as described in Materials and Methods. ONO-1078 was used as a positive control of MRP1 inhibitor.

* $P < 0.05$ versus the control group.